References and Notes

1. B. Patterson and R. Pascual, in *Evolution, Mammals and Southern Continents* (State Univ. of New York Press, Albany, 1972); R. H. Tedford, *Soc. Econ. Paleontol. Mineral. Spec. Publ. No. 21* (1974).
2. E. Feruglio, *Minist. Ind. Commer. Nac. Div. Gen. Yacimientos Pet. Fiscales* **2**, 40 (1949).
3. G. G. Simpson, *Proc. Am. Philos. Soc.* **83**, 655 (1940).
4. R. Pascual, E. J. Ortega Hinojosa, D. Gondar, E. Tonni, *An. Com. Invest. Cient. Prov. Buenos Aires* **6**, 177 (1965).
5. R. Pascual and O. E. Odreman Rivas, *Actas 5th Congr. Geol. Argent.* **3**, 303 (1973).
6. _____, *Ameghiniana* **8**, 375 (1971); R. Pascual, E. J. Ortega Hinojosa, D. Gondar, E. Tonni, in *Paleontografia Bonaerense*, vol. 4, *Vertebrata* (Comision de Investigaciones Cientificas, Province of Buenos Aires, 1966); G. G. Simpson, *Am. Mus. Nat. Hist. Bull.* **91**, 29 (1948); R. Pascual and F. Fidalgo, in *International Colloquium on the Problem "The Boundary between Neogene and Quaternary"* (Moscow, 1972), vol. 2, pp. 231 and 249.
7. J. F. Evernden, D. E. Savage, G. H. Curtis, G. T. James, *Am. J. Sci.* **262**, 170 (1964).
8. B. Patterson, in *Vertebrate Paleontology as a Discipline in Geochronology* (Univ. of California Press, Berkeley, in press).
9. The rock samples dated were of two types: (i) tuffaceous sediments from fossiliferous horizons and (ii) basalts interbedded in tuffaceous fossil horizons or filling channels cut into them. The tuff samples are all fine-grained, often with extensive to total devitrification of the glass. Because they are predominantly water-laid deposits, detrital contamination of the tuffs with older rocks is present in some samples. For these reasons the tuffs are not as reliable as the basalts for radiometric age determinations. The basalts generally show only minor alteration and have given consistent results. Unfortunately, basalts are rare in the stratigraphic sequence, deterring construction of a complete time scale based solely on radiometric age determinations of this rock type.

   Location 1: Near Felton's Estancia. Tuff (KA 1252) collected from Santa Cruz Formation along north bank of Río Gallegos, between Felton's Estancia and Cabo Buen Tiempo, Santa Cruz Province [see (*7*)].

   Location 2: Monte León. Tuff (KA 2944) from Santa Cruz Formation. Sample collected 116 m above contact of Monte León Formation (marine) and overlying Santa Cruz Formation (terrestrial). For stratigraphic section see (*2*, p. 114, figure 133).

   Location 3: Pico Truncado. Samples collected from amphitheater on east side of Pico Truncado. Sample KA 2917 (basalt) was collected from east wall of amphitheater, 37 m above contact of *Pyrotherium* beds (Deseadan horizon) and argiles fissilaires. Basalt overlies Deseadan horizon and corresponds to horizon d of profile 10 in (*26*) and to toba litoidea (*2*, figure 115). Sample KA 2918 is from a second basalt collected 37 m up section from KA 2917, and occurs between horizons e and f of profile 10 in (*26*) and immediately below rodados cuaternarios (*2*, figure 115).

   Location 4: Cerro Blanco. Basalt (KA 2920) is from between Deseadan and Colhuehuapian horizons on west face of Cerro Blanco (*2*, p. 40).

   Location 5: Great Barranca south of Lago Colhué-Huapí. Samples KA 2919 and KA 2942 are from separate isolated channel basalts at west end of Great Barranca (Fig. 2). Both basalts occur between Deseadan and Colhuehuapian horizons; KA 2919 was collected about 100 m northwest of KA 2942. These basalts correspond to manto de teschenita (*2*, figure 104), manto de roca magmatica (*2*, figure 105), and level j, profile 1, in (*26*). Sample KA 2943 is a basalt capping the Deseadan horizon toward the east end of Great Barranca, about 4 km east of the sites where KA 2919 and KA 2942 were collected.

   Location 6: Cerro del Humo. Basalt (KA 2945) capping meseta and directly overlying Mustersan horizon (*Astraponotus* beds). Corresponds to horizon g, profile 6, in (*26*); upper basalt (*2*, figure 117), and basalt in profile 1 and map (*10*, p. 43).

   Location 7: Río Collón Curá. Type locality of Collón Curá Formation, on west bank of Río Collón Curá, on National Route 40, 34 km north of where it crosses National Route 237, Neuquén Province. Ignimbrite lying directly below mammal-bearing tuffaceous horizon was dated.
10. C. R. Vilela, *Minist. Ind. Min. Bull.* **113**, 43 (1971).
11. E. Feruglio, *Bol. Inf. Pet. Yacimientos Pet. Fiscales 171* (1938).
12. R. R. Andreis, M. M. Mazzoni, L. A. Spalletti, *Rev. Asoc. Geol. Argent.* **30**, 86 (1975).
13. G. G. Simpson, *Am. Mus. Novit. 1120* (1938), p. 12.
14. H. H. Camacho, *An. Acad. Nac. Cienc. Exactas Fis. Nat. Buenos Aires* **26**, 46 (1974).
15. A. Bertels, *Rev. Asoc. Geol. Argent.* **25**, 495 (1970).
16. W. A. Berggren and J. A. Van Couvering, *Palaeogeogr. Palaeoclimatol. Palaeoecol.* **16**, figure 1 (1974).
17. L. G. Marshall and R. Pascual, *Mar del Plata Mus. Munic. Cienc. Nat. Publ.* 2, 100 (1976).
18. A. Russo and M. A. Flores, in *Geologia Regional Argentina* (Academia Nacional de Ciencias, Córdoba, 1972).
19. W. B. Scott, *Rep. Princeton Univ. Exp. Patagonia 7* (1932).
20. D. E. Savage, in *Contributions to Primatology* (Karger, Basel, 1975), pp. 2–27.
21. L. G. Marshall, *J. Paleontol.* **50**, 1129 (1976).
22. S. Roth, *Rev. Mus. La Plata* **9**, 381 (1898); *ibid.* **25**, 135 (1920).
23. F. Ameghino, *An. Mus. Nac. Buenos Aires 15* (1906).
24. L. Kraglievich, *Physis* **10**, 127 (1930).
25. P. Groeber, *Dir. Gen. Minas Geol. Hidrol. (Buenos Aires)* **58**, 25 (1929).
26. A. F. Bordas, *An. Mus. Patagonia* **1**, 166 (1945).

27. Funds for fieldwork in Argentina were provided by grant 1329 from the National Geographic Society, Washington, D.C., to L.G.M. The ^{40}K-^{40}Ar dating was supported by NSF grant EAR-00235 A01, formerly GA-40805, to G.H.C.

28 September 1976; revised 12 November 1976

Kinetic Resonance Raman Spectroscopy: Dynamics of Deprotonation of the Schiff Base of Bacteriorhodopsin

Abstract. *We have developed a kinetic technique, combining resonance Raman spectroscopy and variable-speed continuous flow methods, to study molecular dynamics of isolated sites in macromolecules. Kinetic resonance Raman spectra of the retinylidene chromophore of bacteriorhodopsin have been obtained and the dynamics of the deprotonation of the Schiff base linkage is discussed.*

Kinetic studies on reaction intermediates by vibrational spectroscopy have been severely limited, mainly because of the difference in the time scale for most kinetics and the time needed to obtain a vibrational spectrum. Vibrational spectra have, therefore, been obtained on molecular systems either before they are altered or after they have reached a steady state. In this report we describe a kinetic technique that combines resonance Raman spectroscopy and continuous flow methods (*1*, *2*) with variable speeds which allows us to study rapid kinetics of molecular species. We have performed these kinetic experiments on bacteriorhodopsin using all the advantages inherent in vibrational spectroscopy.

In recent years, resonance Raman spectroscopy has become the method of choice for obtaining vibrational spectra of specific sites in macromolecular systems. This is done by selectively enhancing vibrational modes coupled to electronic transitions. When the exciting radiation from a tunable laser is within or near an absorption band, the resonance enhanced spectra are due mainly to the vibrational modes of the chromophore which couples to this absorption band. At Cornell we have used this technique to study the structure and the function of rhodopsins. Rhodopsin is a membrane glycoprotein and is the primary molecule in visual excitation. It absorbs a photon, converting the photonic energy into chemical energy which is used to generate a neural response to the brain (*3*). The active site of all rhodopsins contains the retinylidene chromophore (a form of vitamin A) covalently linked by a Schiff base to the ϵ-amino group of a lysine residue. By selectively enhancing the vibrational spectrum we were able to suggest that the Schiff base linkage in rhodopsin is protonated (*4*). This has been subsequently confirmed by other workers (*2*, *5*). Furthermore, we were also able to show that the Schiff base in bacteriorhodopsin is also protonated and that it can be deuterated (*6*).

Bacteriorhodopsin, which was discovered by Oesterhelt and Stoeckenius (*7*), is contained in the plasma membrane of the bacterium *Halobacterium halobium*. It has been shown that the biological role of bacteriorhodopsin is that of an energy converter. It acts as a light-driven proton pump (*8*), converting light energy into a vectorial proton gradient across the bacterial cell membrane. This proton gradient is used to generate chemical energy in the form of adenosine triphosphate (ATP) when the bacteria are deprived of oxygen. Bacteriorhodopsin and visual pigments are similar in that they not only use the retinylidene chromophore in their photochemically active sites but also have strikingly similar spectral and kinetic properties (*9*, *10*). Bacteriorhodopsin has a well-defined biological role, whereas the biological role of rhodopsin in visual transduction is not known. Thus bacteriorhodopsin, because of its similarities and differences, is an ideal model system to try to elucidate the biological role of visu-

al pigments in generating a neural response.

The photochemical cycle of light-adapted bacteriorhodopsin has been investigated by various workers (*9*) and is summarized in Fig. 1. The first reaction is light driven in the forward and reverse directions, whereas all the other intermediates occur thermally in the dark. It has been shown that batho-bacteriorhodopsin (K_{635}) forms in less than 6 psec (*11*) and decays with a half-time of approximately 2 μsec to L_{550} in the dark. The next intermediate, M_{412}, has a formation time of approximately 40 μsec at room temperature. There are at least one and probably two intermediates present [N(?) and O_{640}] between the decay of M_{412} and the rise of bR_{570}, which occurs in 5 to 10 msec at physiological temperatures. It will become evident that the molecular dynamics of these intermediates can be mapped out with the use of kinetic resonance Raman spectroscopy (KRRS).

The first question we have focused on with this technique is the dynamics of the deprotonation of the Schiff base linkage. Previous experiments in our laboratory had shown that a primary result of the photochemistry of bacteriorhodopsin was the deprotonation of the Schiff base. In fact we demonstrated, using steady state resonance Raman spectroscopy, that M_{412} has an unprotonated Schiff base (*6*). This suggested that the deprotonation of the Schiff base is coupled either directly or indirectly to the proton-pumping mechanisms of bacteriorhodopsin. It is known that the proton gradient forms as a result of the formation of M_{412}. Thus, the formation of M_{412} is crucial to an understanding of how the release of the Schiff base proton initiates a vectorial proton gradient.

Kinetic resonance Raman spectra of bacteriorhodopsin, taken with 30 mw of focused, 457.9-nm laser light for various transit times in the beam (beam diameter divided by bulk flow velocity), are shown in Fig. 2, B–F. The 457.9-nm emission of an argon ion laser was chosen to provide selective enhancement of the M_{412} intermediate. Previous workers have used Raman flow techniques (*2*) in order to obtain the spectrum of rhodopsin with continuous rather than pulsed laser beams. However they excited their samples with low laser powers, with light of frequencies where the absorption cross section was extremely low and without significantly varying the flow velocity. Thus they did not observe the formation and decay kinetics of rhodopsin and its spectral intermediates. On the other hand, we excite the photochemistry and observe the resulting kinetic transformations (see spectra C to F in Fig. 2) by using higher laser powers, by exciting with laser lines near the absorption maxima of the intermediates under investigation, and by varying the flow velocities. In these experiments the bacteriorhodopsin molecules enter the focused (35 ± 3 μm) laser beam in the 570-nm form. Many of these molecules absorb light and begin cycling through the photochemically induced intermediates. Thus the concentrations of the intermediates vary throughout the beam, implying that the observed Raman scattering from any given species is related to the average concentration of that species in the laser beam. Therefore, by varying the flow ve-

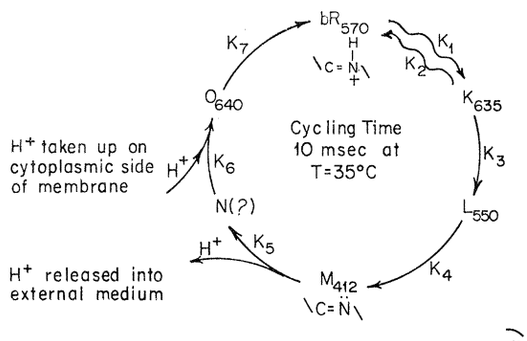

Fig. 1. The proposed photochemical cycle of light-adapted bacteriorhodopsin (*9*). The letters K, L, M, N, O, and bR refer to distinct species, and the numbers to absorption spectra maxima. The absorption maximum of K varies in the literature from 590 to 640 nm.

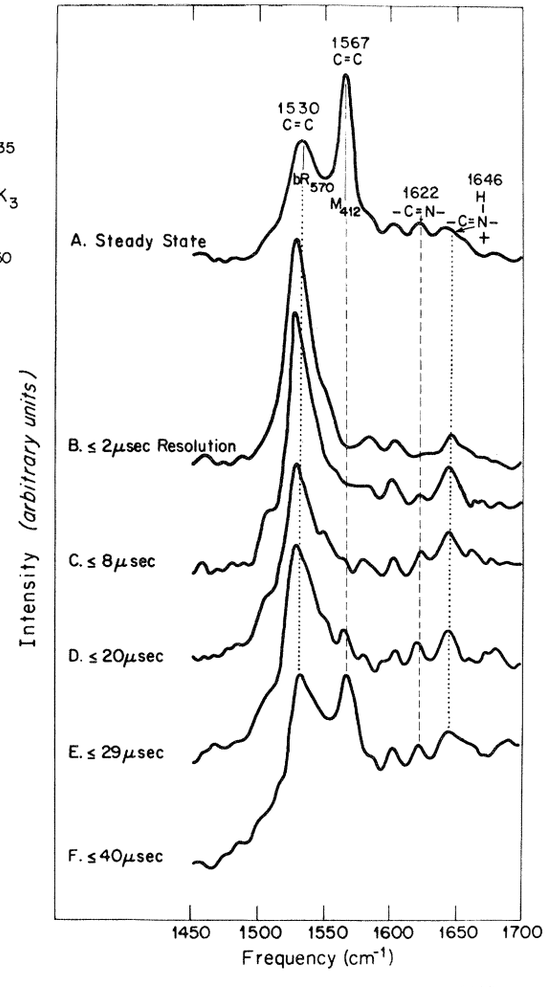

Fig. 2. Steady state and kinetic resonance Raman spectra of bacteriorhodopsin from *Halobacterium halobium* (S9) grown and isolated by the method of Kanner and Racker (*15*). Bacteriorhodopsin (optical density 1.5) was flowed through stainless steel Yale syringe needles of varying diameter by a Cole Parmer masterflex tubing pump and a suitable reservoir to ensure that a bacteriorhodopsin molecule passed through the laser beam only once every few seconds. We excited the vertically flowing bacteriorhodopsin with 30 mw of 457.9-nm light from an argon ion laser focused to a 35 ± 2 μm beam diameter. We measured the beam diameter by translating a razor blade attached to a differential micrometer through the laser beam at its focus, and we used a photodiode as a detector to obtain the profile of the beam. We measured the temperature of the sample to be 29°C with a thermocouple attached to the syringe needle. A JY Ramanor double monochromator with horizontal slits and an RCA C31034 photomultiplier tube were used to collect the 90° scattered light. Photon-counting techniques were employed, and a ModComp II computer was used for data reduction. All data presented were taken with two wave-number steps, a 5-second time constant, and are plotted with arbitrary units. Typically, the largest peak is 2.5 times the background. The spectra shown are only over a limited frequency region. The bands at 1646 cm^{-1} in steady state experiment are shifted to a slightly lower frequency. This is probably due to contributions from other protonated spectral intermediates. The entire spectrum will be reported elsewhere (*13*).

locity we can obtain kinetic resonance Raman spectra with a time resolution of 500 nsec.

In Fig. 2A we show for comparison the spectrum of the same bacteriorhodopsin sample obtained under steady state conditions with identical instrumental settings used to obtain the kinetic spectra shown in Fig. 2, B–F, and the same continuous laser frequency. Previous work in our laboratory and elsewhere showed that the bands at 1530 cm^{-1} and 1567 cm^{-1} in the steady state spectrum (see Fig. 2A) could be ascribed to the C=C stretches for bR_{570} and M_{412}, respectively (*6*, *12*). In addition, we were able to demonstrate that the 1646 cm^{-1} band is due to the protonated Schiff base linkage, and the band at 1622 cm^{-1} is an unprotonated Schiff base linkage (*5*). On the other hand, when the spectrum of bacteriorhodopsin is detected with rapid flow velocities so that the sample is in the laser beam for ≤ 2 μsec, the spectra obtained are identical, an example being shown in Fig. 2B. Notice the absence of bands at 1567 cm^{-1} and 1622 cm^{-1} which have been assigned to M_{412}. This confirms the assignment that the 1530 cm^{-1} and 1646 cm^{-1} bands arise from bR_{570}, a protonated Schiff base (*5*). However, when the time resolution is ≤ 8 μsec (see Fig. 2C), although no band can be detected at 1567 cm^{-1}, there appears to be a small contribution from a band at 1622 cm^{-1}. Also, shoulders appear on either side of the 1530 cm^{-1} peak. These shoulders may be contributions from the C=C stretches of K_{635} and L_{550}, and will be discussed elsewhere (*13*). A spectrum obtained with a resolution of ≤ 20 μsec, as shown in Fig. 2D, still has little contribution from the C=C stretch of M_{412} but shows a larger contribution from the peak around 1622 cm^{-1} as compared to the spectrum with ≤ 8-μsec time resolution. The C=C stretch of M_{412} finally begins to contribute appreciably when the time resolution is ≤ 29 μsec, as is evident from Fig. 2E. Here there is a still larger contribution from the 1622 cm^{-1} band. Finally, at a time resolution of ≤ 40 μsec (Fig. 2F) we have a significantly greater contribution from the C=C stretch of M_{412}, but no significant increase in the intensity of the 1622 cm^{-1} band, the unprotonated Schiff base linkage.

Our data show that the formation time of the 1567 cm^{-1} C=C stretch is consistent with the rate of formation of M_{412} as determined by monitoring the kinetics with absorption spectroscopy (*9*). This is to be expected since it can be shown that the frequency of the C=C stretch of the various intermediates of bacteriorhodopsin is directly correlated with the absorption maximum of the intermediates. However, the 1622 cm^{-1} band begins to appear at least 12 μsec before the first detectable shoulder at 1567 cm^{-1}. One explanation for this observation is that there is another intermediate with an unprotonated Schiff base before M_{412}. Thus the release of the Schiff base proton may be very fast when compared to the detection of a released proton on one side of the membrane (*3*, *14*). This certainly indicates that the release of the Schiff base proton can be only indirectly tied to the proton which is eventually released forming the vectorial proton gradient across the membrane. One possible model [which is consistent with the kinetic data presented herein and the relatively fast deuteration time for the Schiff base proton (our unpublished results)] is to consider the Schiff base proton on the cytoplasmic side of the membrane connected to a series of protein groups with different pK's and exchangeable protons forming a proton-conducting channel which spans the membrane. In such a model the Schiff base proton is only one element in an unidirectional molecular stepladder of exchangeable groups traversing the membrane. Thus the deprotonation of the Schiff base could occur considerably earlier than the ejection of a proton on the outer side of the membrane, as our kinetic data suggest.

In this report we have demonstrated that KRRS is a powerful probe of biomolecular dynamics. Unlike other spectroscopic probes of kinetic transformations (such as fluorescence and absorption spectroscopy), KRRS can provide a much finer detail of time discrimination in specific local regions of a macromolecule. With the development of high-powered tunable dye lasers, and with modelocking and cavity dumping, flow velocities can be considerably reduced and flow volumes can be reduced well beyond the 20-ml (optical density ≈ 1.5) sample used in the experiments we report here. Finally, our interest in the technique results from its applicability to the study of the photonically induced molecular dynamics of the retinylidene chromophore of rhodopsin. There is no reason why rhodopsin cannot be perturbed before the sample is excited by the probing laser beam. In fact, we have started an investigation in our laboratory utilizing a double-beam technique with the exciting beam displaced in time from the probing beam (*13*). By varying the distance between where the two laser beams excite and probe the flowing sample, it becomes possible to obtain resonance Raman spectra of essentially pure kinetic intermediates (*13*). Such information should play a crucial role in helping elucidate the role of rhodopsin in visual transduction and in understanding the molecular basis of the conversion of light energy into chemical energy in bacteriorhodopsin. The technique, however, is not exclusively applicable to rhodopsin and its kinetic intermediates. With the one laser beam that we used, or with two spatially correlated laser beams, KRRS is also generally applicable to a wide variety of other biological systems, such as investigations of various enzymatic reaction mechanisms, analyses of cooperativity in hemoglobin (the kinetic resonance Raman spectra of the heme group could be studied in such systems as carboxyhemoglobin), and observations of molecular dynamics in other photobiological systems.

MICHAEL A. MARCUS
AARON LEWIS
School of Applied Engineering Physics, Cornell University, Ithaca, New York 14853

References and Notes

1. M. D. Hirsch, M. A. Marcus, A. Lewis, H. Mahr, *Biophys. J.* **16**, 1399 (1976); D. Mauzerall, *ibid.*, p. 87; H. Hartridge and F. J. W. Roughton, *Proc. R. Soc. London Ser. A* **104**, 376 (1923), and subsequent references in the last 53 years; W. Woodruff and P. Spiro, *Appl. Spectrosc.* **28**, 576 (1974).
2. R. H. Callender, A. Doukas, R. Crouch, K. Nakanishi, *Biochemistry* **15**, 1621 (1976); R. Mathies, A. R. Oseroff, L. Stryer, *Proc. Natl. Acad. Sci. U.S.A.* **73**, 1 (1976).
3. A. Lewis, *Biophys. J.* **16**, 204a (1976).
4. ———, R. S. Fager, E. W. Abrahamson, *J. Raman Spectrosc.* **1**, 465 (1973); A. Lewis and J. Spoonhower, in *Neutron, X-Ray and Laser Spectroscopy in Biophysics and Chemistry*, S. Yip and S. Chen, Eds. (Academic Press, New York, 1974), p. 347.
5. A. R. Oseroff and R. H. Callender, *Biochemistry* **13**, 4243 (1974).
6. A. Lewis, J. Spoonhower, R. A. Bogomolni, R. H. Lozier, W. Stoeckenius, *Proc. Natl. Acad. Sci. U.S.A.* **71**, 4462 (1974).
7. O. Oesterhelt and W. Stoeckenius, *Nature (London) New Biol.* **233**, 149 (1971); A. Blaurock and W. Stoeckenius, *ibid.*, p. 252.
8. E. Racker and W. Stoeckenius, *J. Biol. Chem.* **249**, 62 (1974); A. Danon and W. Stoeckenius, *Proc. Natl. Acad. Sci. U.S.A.* **71**, 1234 (1974).
9. W. Stoeckenius and R. H. Lozier, *J. Supramol. Struct.* **2**, 759 (1974); N. Dencher and M. Wilms, *Biophys. Struct. Mech.* **1**, 259 (1975); M. C. Kung, D. DeVault, B. Hess, D. Oesterhelt, *Biophys. J.* **15**, 907 (1975); B. Chance, M. Porte, B. Hess, D. Oesterhelt, *ibid.*, p. 913; R. H. Lozier, R. A. Bogomolni, W. Stoeckenius, *ibid.*, p. 955.
10. T. Yoshizawa, in *Handbook of Sensory Physiology*, H. Dartnall, Ed. (Springer-Verlag, Berlin, 1972), vol. 7, part 1, p. 146; E. W. Abrahamson and J. R. Wiesenfeld, in *ibid.*, p. 69.
11. K. J. Kaufmann, P. M. Rentzepis, W. Stoeckenius, A. Lewis, *Biochem. Biophys. Res. Commun.* **68**, 1109 (1976).
12. R. Mendelsohn, *Nature (London)* **243**, 22 (1973).
13. M. A. Marcus and A. Lewis, in preparation.
14. A. Lewis, J. P. Spoonhower, G. J. Perreault, *Nature (London)* **260**, 675 (1976).
15. B. I. Kanner and E. Racker, *Biochem. Biophys. Res. Commun.* **64**, 1054 (1975).
16. We thank E. Racker, E. Labelle, and M. Akabas for assistance in preparing bacteriorhodopsin. We also thank W. Stoeckenius for close and stimulating collaborations. M. A. Marcus is an NIH predoctoral fellow and A. Lewis is an Alfred P. Sloan fellow. This work was supported by grant EY01377 from the National Institutes of Health.

29 June 1976; revised 27 October 1976